
CHAPTER 4 – TEST METHODS

As indicated above, the methodology developed by Nazarian et al. (2003) for quality management of ACP was modified and applied to this study. The test methods employed in that work are introduced in this chapter. A laboratory and a field seismic device were used in this study and compared to traditional laboratory tests. These test methods and the theoretical backgrounds behind them are described below.

PORTABLE SEISMIC PROPERTY ANALYZER

With the PSPA, the average modulus of the exposed surface layers can be estimated within a few seconds in the field. The PSPA, shown in Figure 6, consists of two transducers (accelerometers in this case) and a source packaged into a hand-portable system, which can perform high frequency seismic tests. The source package is also equipped with a transducer for consistency in triggering and for some advanced analysis of the signals. The device is operable from a computer tethered to the hand-carried transducer unit through a cable that carries operational commands to the PSPA and returns the measured signals to the computer.

The operating principle of the PSPA is based on generating and detecting stress waves in a medium. The Ultrasonic Surface Wave (USW) interpretation method, which is implemented in the Spa Manager software in the PSPA computer, is used to determine the modulus of the material. Description of the measurement and implementation techniques is the subject of the next few pages.

To collect data with the PSPA, the technician only initiates the testing sequence through the computer. All the other data acquisition tasks are handled automatically by the computer. The high-frequency source is activated four to six times. Pre-recording impacts of the source are used to adjust the gains of the amplifiers in a manner that optimizes the dynamic range of the electronics. The outputs of the three transducers from the final three impacts are saved and stacked. Typical voltage outputs of the three accelerometers are shown in Figure 7.

The relationship between velocity, V , travel time, Δt , and receiver spacing, ΔX , can be written in the following form:

$$V = \frac{\Delta X}{\Delta t} \quad (4.1)$$

In this equation, V can be the propagation velocity of any of seismic waves [i.e. compression wave, V_P ; shear wave, V_S ; or surface (Rayleigh) wave, V_R]. Knowing any one wave velocity, the modulus can be determined, using appropriate transformations.

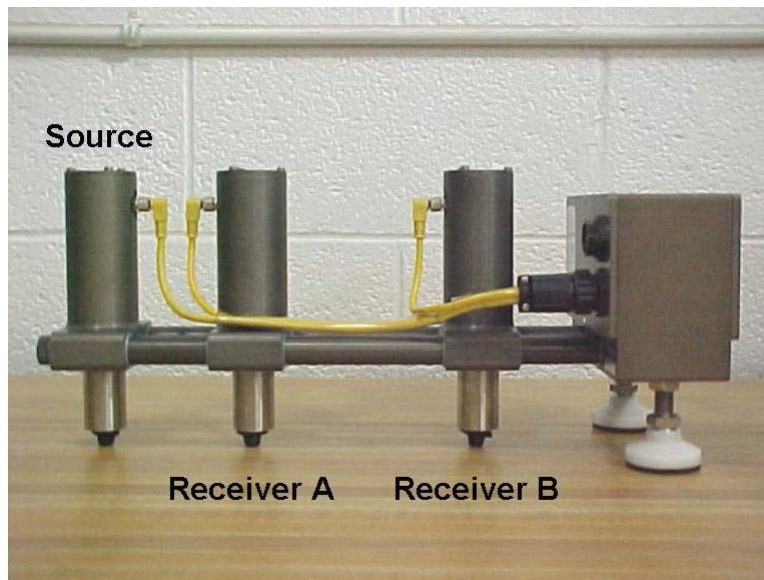
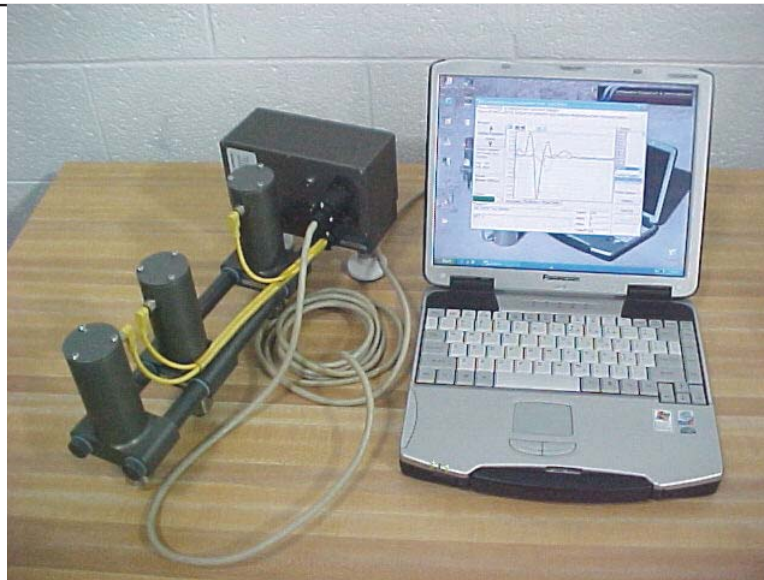


Figure 6. Photo. Portable Seismic Pavement Analyzer.

Shear velocity, V_s can be used to determine shear modulus, G , using:

$$G = \frac{\gamma}{g} V_s^2 \quad (4.2)$$

Young's modulus, E , can be determined from shear modulus, through the Poisson's ratio, ν , using:

$$E = 2(1 + \nu)G \quad (4.3)$$

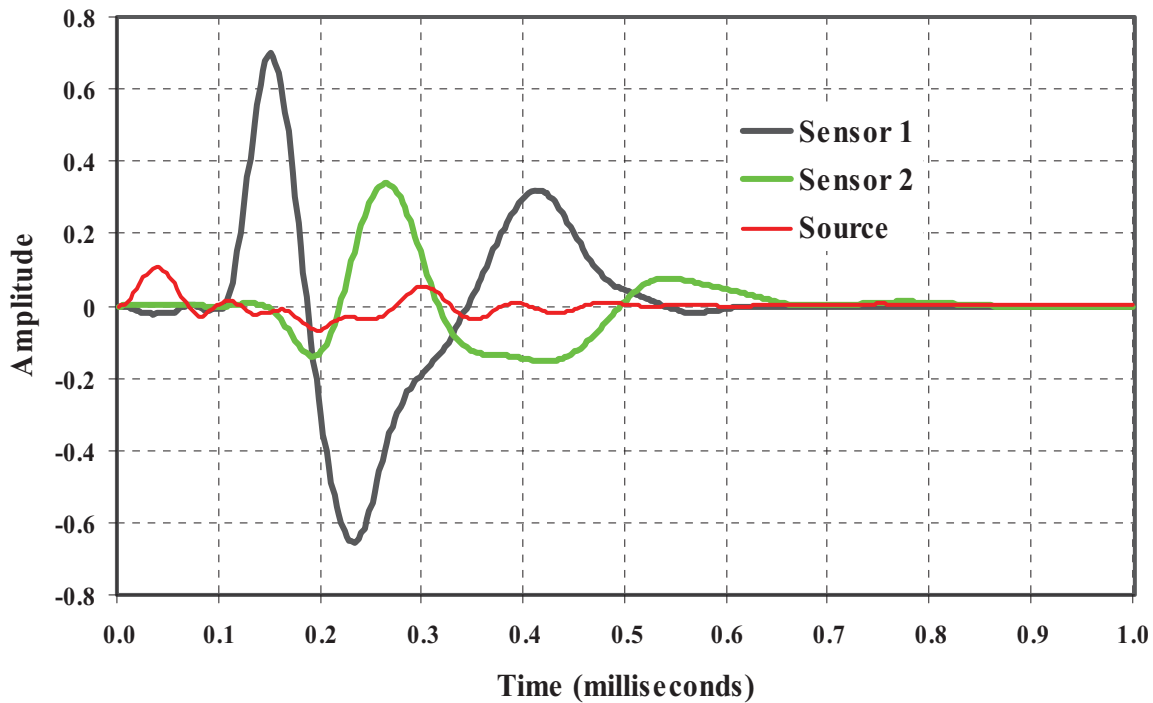


Figure 7. Graph. Typical Time Records from PSPA.

To obtain the modulus from surface wave velocity, V_R is first converted to shear wave velocity using:

$$V_S = V_R (1.13 - 0.16v) \quad (4.4)$$

The shear modulus is then determined by using Equation 4.2.

Surface waves (or Rayleigh, R-waves) contain about two-thirds of the seismic energy. Accordingly, the most dominant arrivals are related to the surface waves making them the easiest to measure. The Ultrasonic Surface Wave (USW) method¹ is an offshoot of the Spectral Analysis of Surface Waves (SASW) method (Nazarian et al., 1997). The major distinction between these two methods is that in the USW method the modulus of the top pavement layer can be directly determined without an inversion algorithm.

As sketched in Figure 8, at wavelengths less than or equal to the thickness of the uppermost layer, the velocity of propagation is independent of wavelength. Therefore, if one simply generates high-frequency (short-wavelength) waves and if one assumes that the properties of the

¹ Some organizations involved in seismic tests do not differentiate between the USW and the SASW methods. In our terminology, the SASW test is a comprehensive test that requires the development of an experimental dispersion curve and determining the modulus profile through an inversion process. The USW simply provides the modulus of the top layer without need for an inversion process and is much simpler to perform.

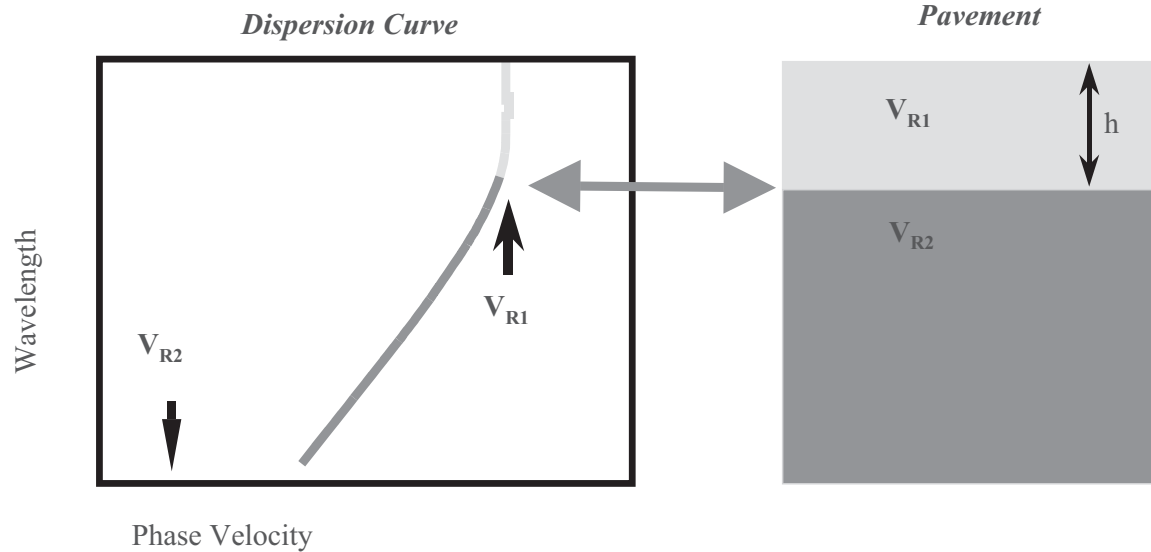


Figure 8. Schematic. Ultrasonic Surface Wave Method.

uppermost layer are uniform, the shear wave velocity of the upper layer, V_s , can be determined from

$$V_s = (1.13 - 0.16\nu) V_{ph} \quad (4.5)$$

The modulus of the top layer, E_{field} , can be determined from

$$E_{field} = 2 \rho V_s^2 (1 + \nu). \quad (4.6)$$

where V_{ph} = phase velocity of surface waves, ρ = mass density, and ν = Poisson's ratio.

The wavelength at which the phase velocity, i.e. velocity of individual frequency components, is no longer constant and closely related to the thickness of the top layer (NCHRP,1996).

Alternatively, the thickness of the ACP layer can be estimated from the impact-echo method as long as the layer is reasonably thick (thicker than 5 in.) and as long as there is enough contrast between the modulus of the ACP and the underlying layer.

An actual dispersion curve from the time record shown in Figure 7 is included in Figure 9a. As approximated by the solid line, the phase velocity is reasonably constant for the first 3 in. below which the phase velocity tends towards lower values with depth. By a comparison of this figure with the idealized one in Figure 8, one can conclude that the average phase velocity is about 4200 fps and the approximate thickness is about 3 in. To obtain the average modulus, the dispersion curve from a wavelength of about 1 in. to slightly less than the nominal thickness of the layer was used.

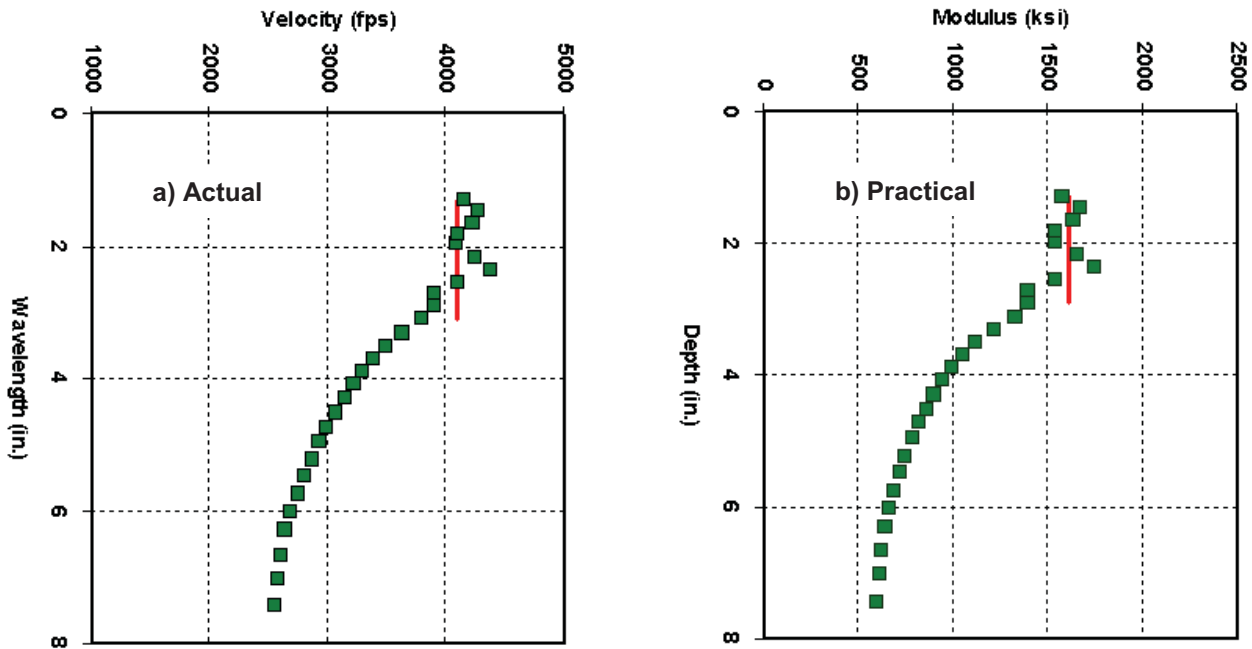


Figure 9. Graph. Typical Dispersion Curve Obtained from Time Records in Figure 7.

For practical inspection of dispersion curve in the field (see Figure 9b), the velocities in Figure 9a are converted to moduli using Equations 4.3 through 4.6, while the wavelength is simply relabeled as depth. In that manner, the operator of the PSPA can get a qualitative feel for the variation in modulus with depth.

The dispersion curve shown in Figure 9 is developed from the phase spectra shown in Figure 10. The phase spectrum, which can be considered as an intermediate step between the time records shown in Figure 8 and the dispersion curve shown in Figure 9 (Nazarian and Desai, 1993), is determined by conducting Fourier transform and spectral analysis on the time records from the two sensors. This step makes the determination of the velocity with wavelength much easier.

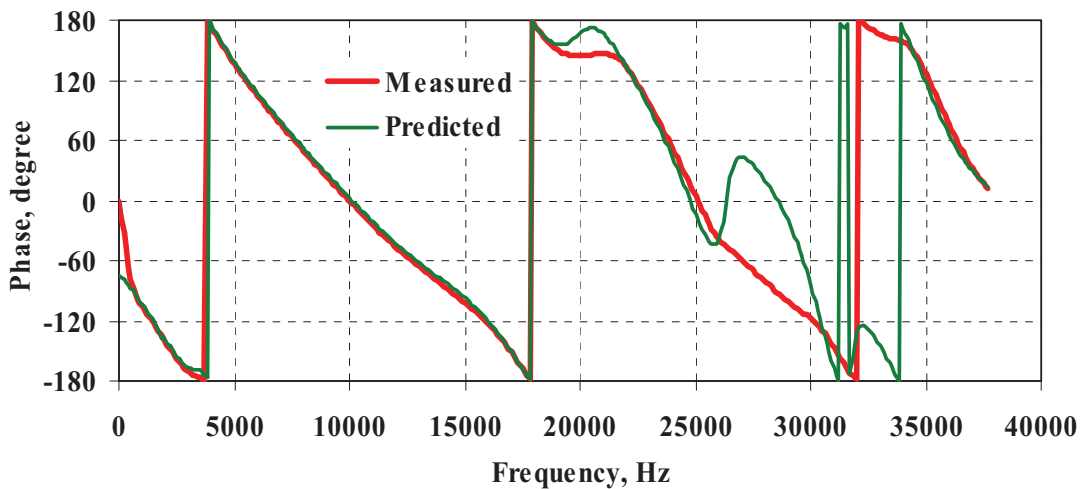


Figure 10. Graph. Typical Phase Spectra Obtained from Time Records in Figure 7.

Two phase spectra are shown, one measured from the time records, and the other that represents the best estimation of the phase when the effect of the body waves are removed. The second one is used to compute the dispersion curve as described above and detailed in Nazarian and Desai (1993).

The Impact Echo method primarily provides information about the thickness of a layer. Sansalone and Carino (1986) have also used the method to locate defects, voids, cracks, and zones of deterioration within concrete. As detailed in Nazarian et al. (1997), the method is not applicable to relatively thin layers and layers where the difference in moduli of adjacent layers is small. In ACP layers, getting accurate estimates of thickness is usually not possible due to scattering around aggregates. The PSPA computes Impact Echo data, but resultant thicknesses are not normally used in ACP applications. Its operation is described here for completeness.

The transducer closer to the source or the one embedded in the source of the PSPA, shown in Figure 6, is used. The method, as sketched in Figure 11, is based on detecting the frequency of the standing wave reflecting from the bottom and the top of the top pavement layer. Upon impact, some of the source energy is reflected from the bottom of the layer, and some is transmitted into the base and subgrade. Since the top of the layer is in contact with air, almost all of the energy is reflected from that interface. The receiver senses the reflected energy at periodic time intervals. The period depends on the thickness and compression wave velocity of the layer. To conveniently determine the frequency associated with the periodic arrival of the signal, one can use a fast Fourier transform algorithm. The frequency associated with the reflected wave appears as a peak in the amplitude spectrum. Using the compression wave velocity of the layer, V_p , the depth-to-reflector, h , can be determined from

$$h = V_p / 2f \tag{4.7}$$

where f is the resonant frequency obtained by transforming the time record into the frequency domain. The compression wave velocity can be determined if the surface wave velocity is known from

$$V_P = V_R [(1 - \nu) / (0.5-\nu)]^{0.5} / (1.13 - 0.16 \nu) \tag{4.8}$$

Since all sites visited for this study contained thin ACP layers, the impact echo results were not used. A new algorithm is currently under development at this time that may enable the reliable detection of the thickness of thin layers.

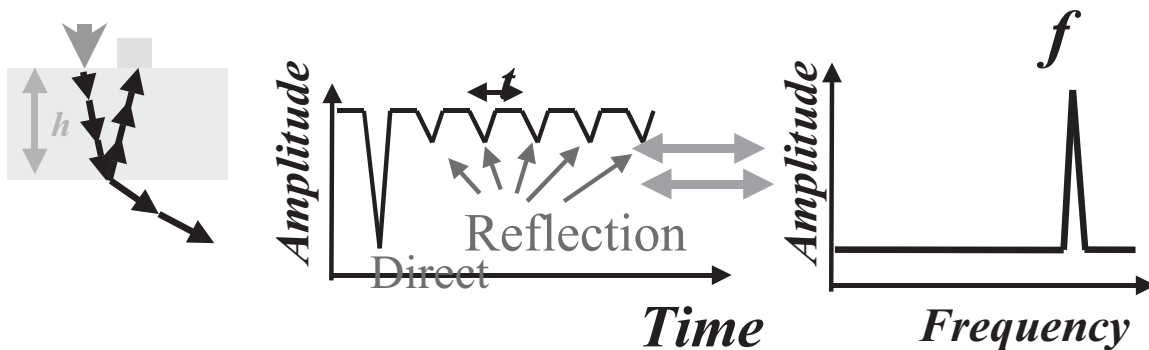


Figure 11. Schematic. Impact Echo Method.

Ultrasonic Laboratory Test

The laboratory setup used in this study is shown in Figure 12. The elastic modulus of a specimen is measured using a device (marketed as a V-meter) containing a pulse generator and a timing circuit, coupled with piezoelectric transmitter. To ensure full contact between the transducers and a specimen, special removable epoxy coupling caps are used on both transducers. To secure the specimen between the transducers, a loading plate is placed on top of it, and a spring-supporting system is placed underneath the transmitting transducer. The compression wave (P-wave) receiving transducer is placed on top of the specimen, on the opposite end from the transmitter. The dominant frequency of the energy imparted to the specimen is 54 kHz. The timing circuit digitally displays the time needed for a wave to travel through and a velocity, V_p , is calculated by dividing the length of the specimen by the corresponding travel time. The modulus, M_v , is then calculated using

$$M_v = \rho V_p^2 \quad (4.9)$$

where ρ is the bulk density of the specimen. For practical use, Equation 4.9 can be rewritten as

$$M_v = \frac{WH}{(\pi R^2 t_v^2)}, \quad (4.10)$$

where W , R and H are the mass, radius and height of the specimen, and t_v = travel time. The size of the sensors used with the test device is large relative to the wave travel path. The modulus measured with the V-meter, M_v , is the so-called constraint modulus. The constraint modulus, M_v can then be converted to Young's modulus, E_v through a theoretically-correct relationship in the form of

$$E_v = M_v \frac{(1+\nu)(1-2\nu)}{(1-\nu)} \quad (4.11)$$

where ν is Poisson's ratio.

DIAMETRAL RESILIENT MODULUS

Measuring resilient modulus is one of the current states of practice for characterizing the modulus of ACP mixtures. This test may be performed either axially or diametrically. Axial resilient modulus tests are conducted on specimens with the length-to-diameter of about two. Because of the sizes of the cores retrieved for this project, only diametral resilient modulus tests could be carried out. ASTM D4123 contains a thorough description of the test procedure.

A picture of a resilient modulus test setup, used in this study, is shown in Figure 13. All tests were carried out with a servo-control dynamic testing device retrofitted in a temperature-controlled chamber.

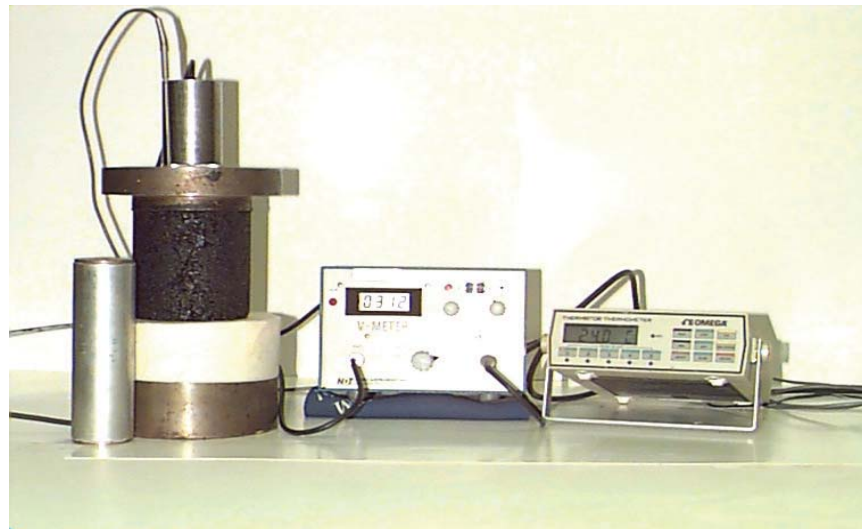
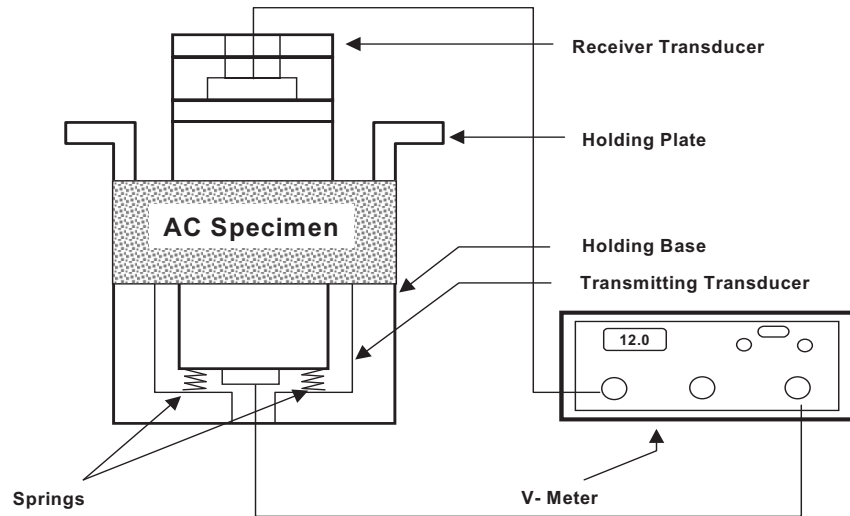


Figure 12. Schematic and Photo. Ultrasonic Test Device for AC Specimens.

A schematic of a specimen being tested is shown in Figure 14. A cyclic compressive load, P , is applied to the specimen vertically along one diameter. This compressive load induces tensile stresses along the diameter of the specimen in line with the load. These tensile stresses cause horizontal deformation of the specimen, ΔH . The resilient modulus of the specimen, E_{RT} is calculated from

$$E_{RT} = P (v + 0.27) / t \quad (4.12)$$

where t = core thickness and v = Poisson's ratio.

A typical load and deformation versus time relationships is shown in Figure 15. The ACP core is subjected to a cyclic haversine deviatoric stress applied for 0.1 seconds followed by a 0.9 sec



Figure 13. Photo. Diametral Resilient Modulus Test.

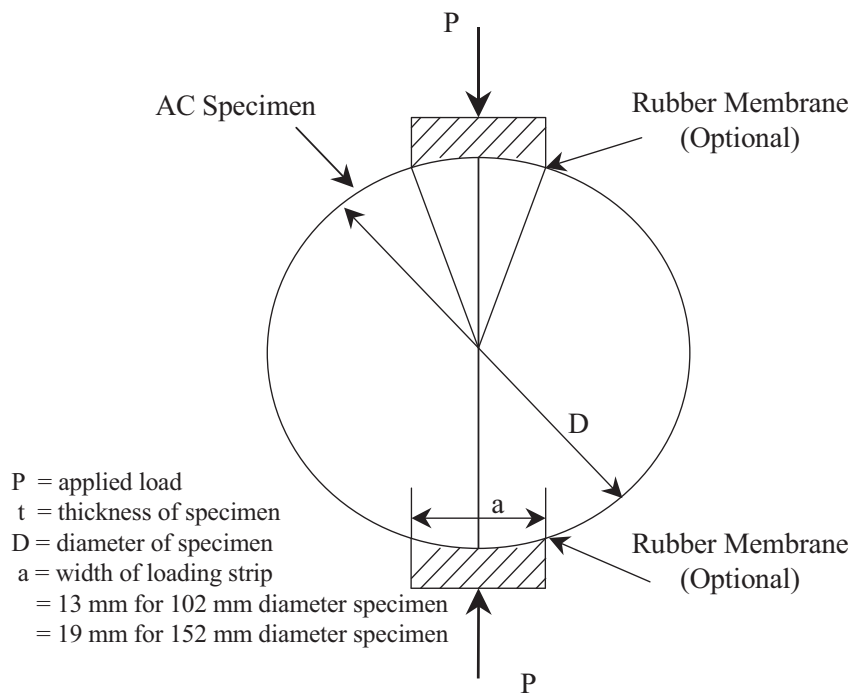


Figure 14. Schematic. Specimen Subjected to Diametral Test.

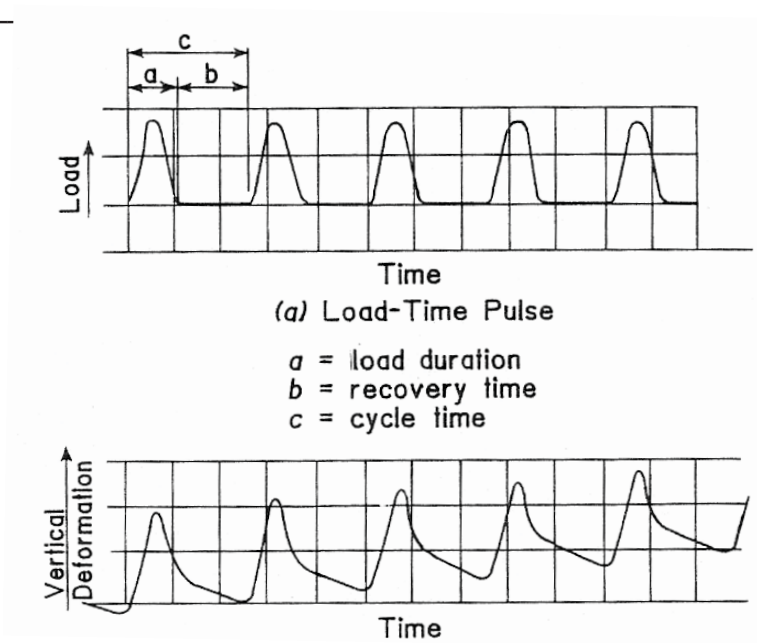


Figure 15. Graph. Time Relationships for Repeated-Load Indirect Tension Test (after Roberts et al., 1996).

rest period. The tests were performed at three temperatures 5 °C, 25 °C, and 45 °C.

At a workshop on resilient modulus testing held at Oregon State University in 1989, there was a strong consensus amongst pavement engineers that the testing procedure is rather time-consuming and results were not very repeatable (Shah, 1993). The estimated repeatability of the test is about 15% to 20%, depending on the sophistication of the test system, and the quality of the cores.